ANTIMICROBIAL AGENTS AND CHEMOTHERAPY, Feb. 2005, p. 708–720 Vol. 49, No. 2
0066-4804/05/$08.00+0 doi:10.1128/AAC.49.2.708–720.2005

Altered NADH/NAD$^+$ Ratio Mediates Coresistance to Isoniazid and Ethionamide in Mycobacteria

Catherine Vilchèze,[1] Torin R. Weisbrod,[1] Bing Chen,[1] Laurent Kremer,[2]† Manzour H. Hazbón,[3] Feng Wang,[4] David Alland,[3] James C. Sacchettini,[4] and William R. Jacobs, Jr.[1]*

Howard Hughes Medical Institute, Department of Microbiology and Immunology, Albert Einstein College of Medicine, Bronx, New York[1]; Laboratoire des Mécanismes Moléculaires de la Pathogénie Microbienne, INSERM, Institut Pasteur de Lille, Lille, France[2]; Division of Infectious Diseases, Department of Medicine, and the Ruy V. Lourenço Center for the Study of Emerging and Reemerging Pathogens, New Jersey Medical School, University of Medicine and Dentistry of New Jersey, Newark, New Jersey[3]; and Department of Biochemistry and Biophysics, Texas A&M University, College Station, Texas[4]

Received 5 August 2004/Returned for modification 9 September 2004/Accepted 27 September 2004

The front-line antituberculosis drug isoniazid (INH) and the related drug ethionamide (ETH) are prodrugs that upon activation inhibit the synthesis of mycolic acids, leading to bactericidal activity. Coresistance to INH and ETH can be mediated by dominant mutations in the target gene *inhA*, encoding an enoyl-ACP reductase, or by recessive mutations in *ndh*, encoding a type II NADH dehydrogenase (NdhII). To address the mechanism of resistance mediated by the latter, we have isolated novel *ndh* mutants of *Mycobacterium smegmatis* and *Mycobacterium bovis* BCG. The *M. smegmatis ndh* mutants were highly resistant to INH and ETH, while the *M. bovis* BCG mutants had low-level resistance to INH and ETH. All mutants had defects in NdhII activity resulting in an increase in intracellular NADH/NAD$^+$ ratios. Increasing NADH levels were shown to protect InhA against inhibition by the INH-NAD adduct formed upon INH activation. We conclude that *ndh* mutations mediate a novel mechanism of resistance by increasing the NADH cellular concentration, which competitively inhibits the binding of INH-NAD or ETH-NAD adduct to InhA.

Despite the declaration by the World Health Organization 10 years ago that tuberculosis (TB) was a global health emergency, the problem has worsened primarily due to the growing human immunodeficiency virus epidemic and the emergence of drug resistance (9, 12). Although TB can be cured by a regimen of several drugs for at least 6 months, the emergence of drug-resistant and multidrug-resistant TB has created new challenges to control and defeat the disease. According to the World Health Organization, drug-resistant *Mycobacterium tuberculosis* strains are found in at least 72 countries at a rate ranging from 3 to 41% (53). Understanding the mechanisms by which drug resistance occurs is important in order to quickly identify drug-resistant strains to treat the patients adequately. Moreover, knowledge of resistance mechanisms leads to the understanding of the mode of drug action and to the development of strategies to overcome drug resistance.

Isoniazid (INH) is one of the most effective drugs used to treat TB. INH was introduced as an antituberculosis drug in 1952 (4, 13) and, soon after, the first INH-resistant (INH^r) *M. tuberculosis* strains were isolated (35). It is estimated that worldwide up to 28% of the *M. tuberculosis* strains are INH^r, with a median of 6.2% in new TB cases (53). In previously treated TB cases, the percentage of INH^r strains can reach up to 60% (53).

Numerous genes have been found to be associated with INH resistance in clinical isolates (43). However, to date only two genes, *katG* encoding a catalase peroxidase and *inhA* encoding an NADH-dependent enoyl-ACP reductase, have been shown to confer greater than fivefold increased susceptibility or resistance to *M. tuberculosis* upon gene transfer (26, 56). Mutations in *katG* are recessive, resulting in a loss or altered catalase peroxidase function (and subsequent INH resistance) in both INH^r laboratory-isolated mutants and INH^r clinical isolates (17, 22, 27, 41, 43, 57). The recessive nature of the *katG* mutations, i.e., the restoration of catalase peroxidase activity and INH susceptibility when replaced or complemented with the wild-type gene, is consistent with the fact that KatG activates INH (20, 56, 57) to generate a hypothetical isonicotinic acyl radical that reacts with NAD and forms an INH-NAD adduct (45). This adduct binds to and inhibits InhA (29, 40, 44, 45, 52), resulting in mycolic acid biosynthesis inhibition (49) and cell death (49, 51). In contrast, overexpressed *inhA* alleles or alleles causing amino acid substitutions within the structural gene have been shown to confer INH resistance in a dominant fashion, i.e., conferring INH resistance when the mutant alleles replace or complement the wild-type gene (1, 26, 51). Mutations in INH^r clinical isolates of *M. tuberculosis* have been mapped to the promoter region or the structural gene of *inhA* (1, 2, 17, 22, 27, 31, 38, 41, 43). The dominant nature of these mutations was consistent with the hypothesis that *inhA* encodes the target of INH (1, 23, 26).

The structural analog of INH, ethionamide (ETH), another InhA inhibitor, has provided important insights into INH action. Early studies of clinical strains resistant to INH revealed that some of the strains were also coresistant to ETH and/or thiosemicarbazone, even though the patients had never been treated with those drugs (6, 7, 18, 28). A recent study of 41 ETH-resistant (ETH^r) clinical isolates of *M. tuberculosis* demonstrated that most of the strains were also coresistant to INH

* Corresponding author. Mailing address: Howard Hughes Medical Institute, Department of Microbiology and Immunology, Albert Einstein College of Medicine, Bronx, NY 10461. Phone: (718) 430-2888. Fax: (718) 518-0366. E-mail: jacobsw@hhmi.org.

† Present address: Dynamique des Interactions Membranaires, CNRS UMR 5539, Université de Montpellier II, 34095 Montpellier, France.

and that, in 51% of these strains, the ETH^r and INH^r phenotypes were solely due to mutations in the *inhA* gene and/or its promoter region (38). Mutations in *inhA* or overexpression of *inhA* have previously been shown to confer resistance in a dominant fashion to ETH and INH (1, 26). Like INH, ETH appears to be a prodrug that is activated by the monooxygenase EthA (3, 10, 14, 50). An ETH-NAD adduct had been hypothesized to be the inhibitor of InhA (45).

Coresistance to INH and ETH has also been shown to be mediated in a recessive fashion in *Mycobacterium smegmatis* by mutations in *ndh*, a gene encoding a type II NADH dehydrogenase (NdhII) (36). The orthologue NdhII protein has been characterized in *Escherichia coli* as a membrane-bound, monomeric, non-proton-translocating flavoprotein that oxidizes NADH, reduces quinone, and catalyzes the transfer of electrons from the reduced flavin to quinones (15, 19, 21, 32, 54). The *M. tuberculosis* genome contains genes encoding both NdhII (*ndh*; Rv1584c) and the type I NADH dehydrogenase (NdhI) (*nuoA-N*; Rv3145 to -3158). The orthologue NdhI protein has been characterized in *E. coli* as a membrane-associated, multimeric, energy-coupling, proton-translocating enzyme that oxidizes NADH and pumps protons across the membrane using the energy generated by the redox reaction (15, 21, 54, 55). Mutations in *ndh* have been identified in INH^r clinical isolates of *M. tuberculosis* (27), but no complementation experiments were done to show that the INH resistance phenotype was due to the *ndh* mutation in those strains and the level of ETH resistance was not measured. Therefore, to demonstrate that *ndh* mutations can cause INH and ETH resistance in slow-growing mycobacteria and to elucidate the mechanism of INH and ETH resistance due to *ndh* mutations in mycobacteria, we sought to isolate spontaneous *ndh* mutants in fast- and slow-growing mycobacteria. In this report, we describe the isolation and genetic characterization of spontaneous *ndh* mutants in *M. smegmatis* and *Mycobacterium bovis* BCG. In addition, we analyze the NdhII activity and the resulting NADH/NAD$^+$ ratios in the INH and ETH coresistant mutants and propose a new mechanism for INH and ETH resistance in mycobacteria.

MATERIALS AND METHODS

Bacterial strains, plasmids, and media. The *M. smegmatis*, *M. bovis* BCG, and *M. tuberculosis* H37Rv mutants were obtained from laboratory stocks. The plasmids used in this study were described previously (26, 36). The *M. smegmatis* strains were grown in Middlebrook 7H9 medium (Difco) supplemented with 10% (vol/vol) ADS enrichment (50 g of albumin, 20 g of dextrose, 8.5 g of sodium chloride in 1 liter water), 0.2% (vol/vol) glycerol, and 0.5% (vol/vol) Tween 80. The *M. bovis* BCG and *M. tuberculosis* H37Rv strains were grown in Middlebrook 7H9 medium (Difco) supplemented with 10% (vol/vol) OADC enrichment (Difco), 0.2% (vol/vol) glycerol, and 0.05% (vol/vol) Tween 80. The solid medium used was the same as that described above with the addition of 1.5% (wt/vol) agar.

Isolation of spontaneous mutants. Mutants were isolated from nonmutagenized cultures grown in the media described above. The cultures were incubated with shaking at 30°C for *M. smegmatis* and at 37°C for *M. bovis* BCG and *M. tuberculosis* H37Rv until they reached an optical density at 600 nm (OD_{600}) of at least 1.0. Tenfold serial dilutions were then plated on agar plates (media described above) containing either INH (25 μg/ml) for *M. smegmatis* mutant isolation or INH (0.25 μg/ml) and ETH (5 or 10 μg/ml) for *M. bovis* BCG and *M. tuberculosis* H37Rv mutant isolation. The plates were then incubated at 30°C for 7 days for *M. smegmatis* mutant isolation or at 37°C for 4 to 6 weeks for *M. bovis* BCG and *M. tuberculosis* H37Rv mutant isolation.

Assessment of Ts lethality phenotype. The *M. smegmatis ndh* mutants were grown to stationary phase at 30°C. Tenfold serial dilutions were plated onto two sets of plates: one set was incubated at 30°C for 7 days (for titration of the cultures) and the other set was incubated at 42°C for 5 days. The plates incubated at 42°C were then shifted to 30°C, and the incubation continued for 7 days. A strain was considered to have a temperature-sensitive (Ts) lethal phenotype if less than 10% of its population could survive the incubation at 42°C (measured by the number of CFU per milliliter obtained after 5 days at 42°C followed by 7 days at 30°C divided by the titer).

MIC determination. Mycobacterial cultures were grown to an OD_{600} of ≈1.0. Tenfold serial dilutions were plated on plates containing the following drug concentrations: for *M. smegmatis* strains, INH (0, 5, 10, 25, 50, 100 μg/ml), ETH (0, 5, 10, 25, 50, 100 μg/ml), triclosan (TRC; 0, 5, 10, 15, 25, 50 μg/ml), streptomycin (0.1, 0.25, 0.5, 1 μg/ml), ethambutol (0.1, 0.25, 0.5, 1, 5 μg/ml), and rifampin (5, 10, 25, 50, 75, 100 μg/ml); for *M. bovis* BCG strains, INH (0, 0.1, 0.2, 0.25, 0.3, 0.4, 0.5, 0.6, 0.8, 1 μg/ml), ETH (0, 2.5, 5, 10, 12.5, 15, 20 μg/ml), and TRC (0, 5, 10, 12.5, 15, 20 μg/ml). The MIC was determined as the concentration of drug that reduced the number of CFU per milliliter by 99%.

PCR amplification. The *ndh* gene was amplified from chromosomal DNA using the following primers: for *M. smegmatis*, TW96 (5′-CGAGGAGCATCA ATGAGCCA-3′) and TW97 (5′-CTCGACCGAACCGGCTAGGA-3′); for *M. bovis* BCG, TW539 (5′-CTGACCGGTTGGCTGGTAA-3′) and NDHB2 (5′-CGGATCCAGCAGCGGAACATGAG-3′). The products were directly sequenced bidirectionally, and the sequences were aligned against each other and the wild-type sequence.

Transformation experiments. *M. smegmatis* strains (10-ml cultures) were grown at 30°C to mid-log phase (OD_{600} ≈ 0.7), washed twice with 10% cold glycerol, and resuspended in cold 10% glycerol (0.5 ml). To perform transformations, the cold cell suspension (150 μl) was added to the plasmid (1.5 μl) and then electroporated using the following parameters: 2.5 V, 25 μF, and 1,000 Ω. Medium (1 ml) was added to the suspension, which was incubated at 30°C for 5 h, and then plated. For *M. bovis* BCG strains, the same protocol was followed, but cell preparation and electroporation were performed at room temperature and incubation was done at 37°C (25).

NADH dehydrogenase assays. Cultures (500 ml) were grown to mid-log phase (OD_{600} ≈ 0.7), spun down, and washed twice in cold phosphate buffer (50 mM K_2HPO_4 [pH 7.5], 5 mM $MgSO_4$). The cell pellet was weighed and resuspended in cold phosphate buffer (1 ml/g of pellet). DNase and proteinase inhibitors were added to the cell suspension, and the cells were broken using a French press (four passages; 1,000 lb/in^2/cm^2). The cell debris was removed by centrifugation (12,000 × *g*, 20 min), and the membrane fraction was isolated by ultracentrifugation (100,000 × *g*, 90 min). The membrane fraction was then resuspended in phosphate buffer, and protein concentration was measured using the Bio-Rad protein assay. NADH dehydrogenase activities (type I and II) were assayed spectrophotometrically, in the membrane fractions, at room temperature, by measuring the rate of NHDH (reduced nicotinamide hypoxanthine dinucleotide) oxidation at 340 nm (type I) or the rate of NADH oxidation in the presence of menadione (2 mM) at 340 nm (type II), or by measuring the rate of 2,6-dichloroindophenol (DCIP) reduction at 610 nm in the presence of NHDH (type I) or NADH (type II) (36).

Determination of NADH and NAD$^+$ cellular concentrations. Mycobacterial cultures were grown to an OD_{600} ranging from 0.8 to 1.2. A sample of the cultures (1 ml) was spun, and the cell pellets were resuspended in 0.2 M HCl (0.3 ml, NAD$^+$ extraction) or 0.2 M NaOH (0.3 ml, NADH extraction). After 10 min at 55°C, the suspensions were cooled to 0°C and neutralized by adding 0.1 M NaOH (0.3 ml, NAD$^+$ extraction) or 0.1 M HCl (0.3 ml, NADH extraction) while vortexing at high speed. After centrifugation, the supernatants were collected and transferred to a new tube and used immediately. The concentration of NAD$^+$ (or NADH) was obtained by measuring spectrophotometrically the rate of 3-[4,5-dimethylthiazol-2-yl]-2,5-diphenyltetrazolium bromide reduction by the yeast type II alcohol dehydrogenase in the presence of phenazine ethosulfate at 570 nm (30, 46). The rate of 3-[4,5-dimethylthiazol-2-yl]-2,5-diphenyltetrazolium bromide reduction is proportional to the concentration of nucleotide.

Quantification of the *inhA* expression levels. Total RNA extractions, cDNA synthesis, and quantitative PCR with molecular beacons were performed as described previously (26).

Western blot analysis. *M. bovis* BCG mid-log-phase cultures (10 ml) were resuspended in 0.8 ml of phosphate buffer (phosphate-buffered saline; 20 mM K_2HPO_4 [pH 7.5], 0.15 M NaCl) and disrupted during 10 min using a Branson Sonifier 450. Equal amounts of protein (25 μg/lane) were then separated on a sodium dodecyl sulfate–12% polyacrylamide gel as described previously (24). After electrophoresis, the proteins were transferred onto a Hybond-C Extra membrane (Amersham). Membranes were then saturated with 2% dry milk in

TABLE 1. Characterization of *M. smegmatis ndh* mutants

Strain	*ndh* allele	Mutation		MIC (μg/ml)			% Viability at 42°C[a]
		DNA	Amino acid	INH	ETH	TRC	
mc^2155	*ndh*	Wild type	Wild type	5	10	10	100
mc^2374	*ndh-64*	T50C	I17T	>100	>100	25	55
mc^2375	*ndh-52*	A85C	T29P	>100	50	10	31
mc^2376	*ndh-101*	A137C	H46P	>100	>100	25	99
mc^2377[g]	***ndh-61***	**G251A**	**G84D**	**>100**	**>100**	**25**	**1**
mc^2378	***ndh-11***	**T299C**	**L100P**	**100**	**>100**	**10**	**1**
mc^2379	*ndh-16*	G343A[b]	A115T	>100	>100	25	10
mc^2380	*ndh-13*	T364A	Y122N	>100	>100	25	10
mc^2381	***ndh-32***	**C433T[c]**	**R145C**	**>100**	**>100**	**25**	**1**
mc^2382	*ndh-41*	T509C	F170S	>100	>100	10	45
mc^2383	*ndh-23*	G559C[d]	A187P	50	50	25	12
mc^2384	*ndh-71*	T737C	V246A	>100	>100	10	30
mc^2385	*ndh-17*	T815A	V272E	>100	>100	10	46
mc^2386	*ndh-22*	T899G[e]	V300G	>100	>100	25	30
mc^2387	*ndh-31*	G1005T	Q335H	100	100	10	35
mc^2388	*ndh-84*	T1081C[f]	Y361H	>100	100	10	50

[a] Viability at 42°C was defined as the percentage of cells that survived incubation at 42°C. Ten- fold serial dilutions of mycobacterial cultures were plated at the nonpermissive temperature (42°C). After incubation at 42°C for 4 days, the plates were incubated at the permissive temperature (30°C) for 6 days. The number of CFU per milliliter obtained after the temperature shift was divided by the titer of the culture to give the percent viability at 42°C.
[b] Also found in mutant *ndh-18.* This was the only mutation previously isolated (36).
[c] Also found in mutants *ndh-63* and *ndh-93.*
[d] Also found in mutant *ndh-12.*
[e] Also found in mutants *ndh-24, ndh-51,* and *ndh-83.*
[f] Also found in mutants *ndh-62, ndh-81, ndh-82,* and *ndh-85.*
[g] The *M. smegmatis ndh* Ts lethal mutants are shown in bold.

phosphate-buffered saline–0.1% Tween 20 and incubated overnight with rabbit anti-InhA antibodies raised against the *M. tuberculosis* InhA protein (23) (dilution, 1/30,000). Membranes were then washed and incubated with anti-rabbit antibodies conjugated to alkaline phosphatase (1/7,000 dilution; Promega).

InhA enzymatic activity assay. All assays were carried out on a Cary 100 Bio Spectrophotometer by monitoring oxidation of NADH at 340 nm. The *M. tuberculosis* InhA protein was expressed and purified as previously described (42). Three different procedures were used to assay the activity of *M. tuberculosis* InhA with increasing concentration of NADH. In the first experiment, the INH-NAD adduct was presynthesized by adding Mn(III) pyrophosphate (4 mM) into a mixture consisting of INH (2 mM) and NAD^+ (2 mM) in 100 mM potassium phosphate buffer solution, pH 7.5 (40). The assay was performed by incubating InhA (60 nM) with increasing concentrations of NADH (10, 100, or 500 μM or 1 mM) and the INH-NAD adduct solution (10 μM) for 20 min in 100 mM potassium phosphate buffer solution, pH 7.5 (40). The reaction was initiated by adding 2-*trans*-dodecenoyl-coenzyme A (CoA) (50 μM). In the second assay, InhA (60 nM) was mixed together with NADH (10, 100, or 500 μM or 1 mM), INH (10 μM), and Mn(III) pyrophosphate (20 μM) in 100 mM potassium phosphate buffer solution, pH 7.5, and the reaction was initiated by adding 2-*trans*-dodecenoyl-CoA (50 μM). In the third experiment, the INH-NAD adduct was presynthesized (as described for the first experiment) and incubated with InhA (5 μM) for 3 h, followed by separation using a Hi-Trap (5-ml) desalting column. The InhA-inhibitor complex was collected and assayed as in the first experiment.

RESULTS

Isolation of novel *ndh* mutants in *M. smegmatis*. We have previously shown that spontaneous *M. smegmatis ndh* mutants could be isolated by plating nonmutagenized *M. smegmatis* cultures onto rich medium (Mueller-Hinton) plates containing INH (25 μg/ml; five times the MIC), incubating the plates at 30°C, and then screening for the mutants that failed to grow at 42°C (36). These mutants were found to have pleiotropic mutations in *ndh* conferring four independent phenotypes: INH resistance, ETH resistance, temperature sensitivity, and auxotrophy. In an attempt to identify novel alleles mapping to *ndh* involved in INH resistance, we isolated spontaneous INH^r mutants by plating 10-fold serial dilutions of 10 independent, nonmutagenized *M. smegmatis* cultures onto minimal medium Middlebrook 7H10 plates containing 25 μg of INH/ml. INH^r mutants were isolated at a frequency ranging from 8×10^{-7} to 9×10^{-8}. When screening for thermosensitivity, 6 to 18% of these mutants were temperature sensitive for growth at 42°C. We isolated 26 mutants that were INH^r Ts and prototrophs.

The mutants were highly resistant to INH (MIC ≥ 50 μg/ml, with most of the mutants being resistant to more than 100 μg/ml) (Table 1) but were susceptible to other antimycobacterial drugs, like streptomycin, ethambutol, and rifampin (data not shown). Two other antimycobacterial agents, ETH and TRC, both targeting InhA (1, 34), were also tested. As shown in Table 1, the *M. smegmatis* mutants were highly resistant to ETH but had a low resistance to TRC.

To test if the mutations mapped to *ndh*, the INH^r Ts mutants were transformed with pYUB803, an extrachromosomal plasmid (pMV261 [48]) containing the *M. smegmatis ndh* gene, and the resulting transformants were screened for loss of thermosensitivity and INH resistance. The pYUB803 construct restored INH sensitivity and temperature resistance phenotypes to all the INH^r Ts mutants (data not shown). Furthermore, pYUB808, a replicative plasmid (pMV261) containing the *M. bovis* BCG *mdh* gene encoding the NADH-dependent malate dehydrogenase, also restored thermoresistance in all but one mutant (mc^2380) (data not shown). Although *M. smegmatis* does not possess the NADH-specific malate dehydrogenase, Miesel et al. (36) had shown that the *M. bovis* BCG *mdh* gene was able to restore wild-type phenotypes to *M. smegmatis ndh* mutants. Interestingly, Molenaar et al. (37) postulated that Mdh allows for the restoration of the Ndh enzymatic activity by combining with the *M. smegmatis* malate: quinone oxidoreductase (Mqo) enzyme. Taken together, these transformation studies were consistent with the hypothesis that

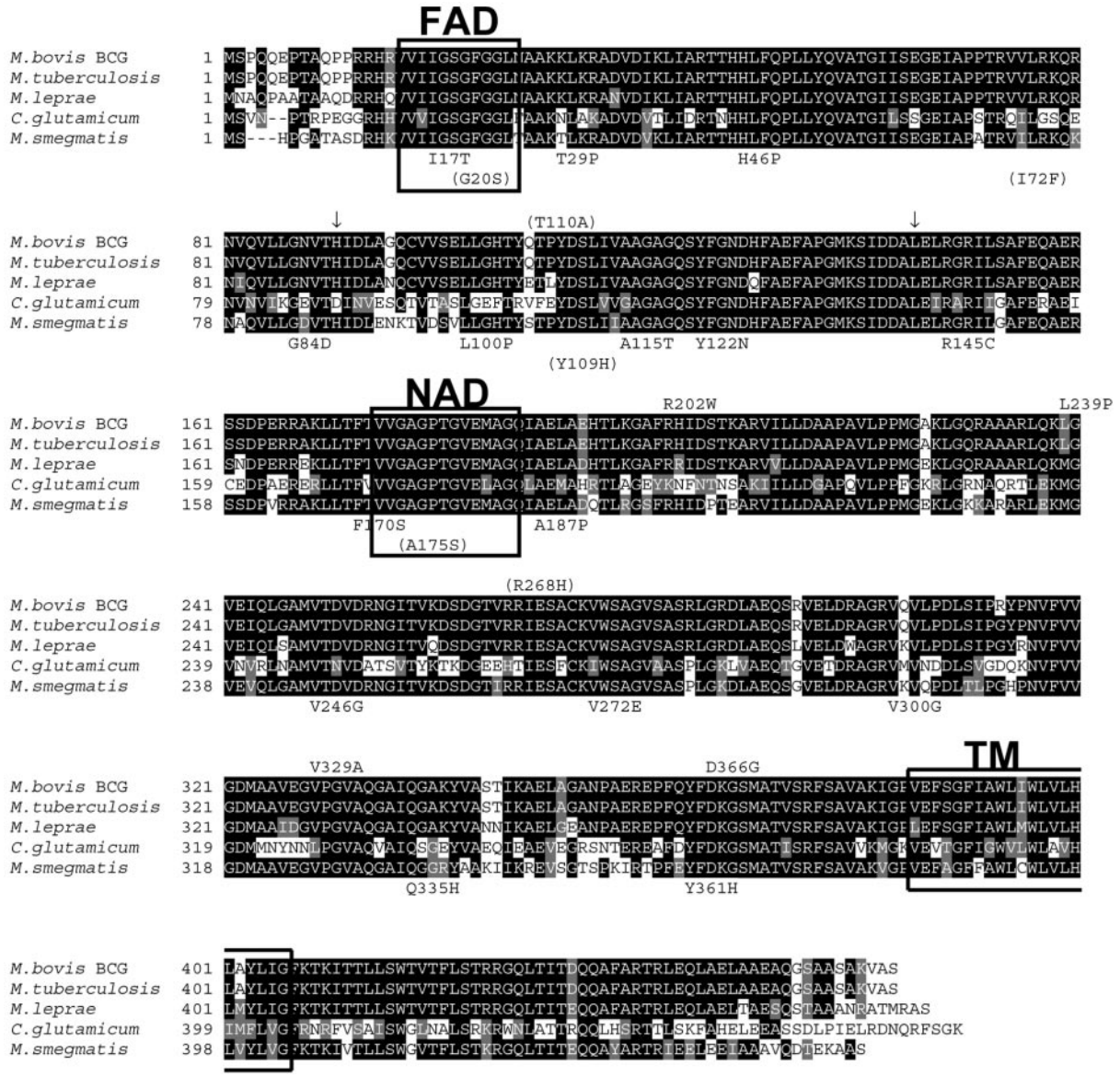

FIG. 1. Sequence alignment of actinomyces NdHII proteins and mutation descriptions. The NdhII proteins from *M. bovis* BCG, *M. tuberculosis, M. leprae*, *Corynebacterium glutamicum*, and *M. smegmatis* were aligned using BOXSHADE 3.21 (http://www.ch.embnet.org/software/BOX_form .html). The putative FAD and NAD binding motifs (33) and transmembrane domain (TM) (http://www.cbs.dtu.dk/services/TMHMM/) (47) are boxed, and the conserved regions have a black background. The positions and the amino acid substitutions found in *M. smegmatis ndh* mutants isolated in this study and in previous studies (in parentheses) (36) are shown below the *M. smegmatis* alignment. The positions and the amino acid substitutions found in *M. bovis* BCG *ndh* mutants isolated in this study are shown above the *M. bovis* BCG alignment (the base pair insertions are indicated with arrows), while the positions and the amino acid changes previously isolated in *M. tuberculosis* clinical isolates (27) are shown in parentheses above the *M. bovis* BCG alignment.

all the mutants had acquired mutations in the *M. smegmatis ndh* gene.

Sequence analysis revealed that all 26 mutants contained single point mutations in the *ndh* gene resulting in amino acid substitutions (Table 1). Eleven of the mutations were found more than once. The G559C (Ala187Pro) and T1081C (Tyr361His) mutations were found in two independent cultures, whereas the C433T (Arg145Cys) and T899G (Val300Gly) mutations were found in three independent cultures. Thus, of the 15 unique mutations identified, only 1, the Ala115Thr amino acid change, had been isolated previously and it, too, was found to be a prototroph (36). The locations of the amino acid substitutions caused by the mutations are depicted on the protein sequence (Fig. 1). The *M. smegmatis ndh* gene is 1,374 bp in length, encoding an open reading frame of 458 amino acids. All of the mutations caused amino acid substitutions from amino acid 17 to amino acid 361 (Fig. 1). None of the mutations was positioned in the NAD binding site and only one (Ile17Thr) was located in the FAD binding site, but most of the mutations were found in conserved regions of Ndh from *M. tuberculosis*, *Mycobacterium leprae*, and *Corynebacterium glutamicum* (Fig. 1).

Coresistance to INH and ETH can be mediated by *ndh* mutations in *M. bovis* BCG. Since *M. smegmatis* is 100 times more resistant to INH than *M. tuberculosis* or *M. bovis* BCG is,

TABLE 2. Characterization of *M. bovis* BCG Pasteur *ndh* mutants

Strain	*ndh* allele	Mutation		MIC (μg/ml)		
		DNA	Amino acid	INH	ETH	TRC
BCG Pasteur	*ndh*	Wild type	Wild type	0.1	2.5	5
mc^{2}2402	*ndh-3*	insbp272(a)[a]	Frameshift	0.3	15	15
mc^{2}2403	*ndh-443*	insbp439(t)	Frameshift	0.6	15	10
mc^{2}2404	*ndh-44*	C604T	R202W	0.3	10	10
mc^{2}2400	*ndh-33*	T716C	L239P	0.25	12.5	12.5
mc^{2}2401	*ndh-38*	T986C	V329A	0.25	10	15
mc^{2}2405	*ndh-55*	A1097G	D366G	0.3	20	10

[a] insbp272(a) refers to insertion base pair a at position 272.

we addressed whether *ndh* mutations could confer resistance to INH and ETH in slow-growing mycobacteria. Interestingly, a previous study identified mutations in *ndh* in INH^r *M. tuberculosis* clinical isolates from Singapore, although no gene transfers were performed to prove that the resistance was directly mediated by the *ndh* mutations (27). Here, *M. bovis* BCG Pasteur was chosen with the intention of facilitating safety containment during French press procedures required for biochemical analyses. To enrich for *ndh* mutants and to eliminate the eventual selection of INH^r strains carrying mutations within the *katG* gene, we isolated spontaneous mutants of *M. bovis* BCG resistant to both INH and ETH. The INH^r and ETH^r mutants were obtained by plating 10-fold serial dilutions of three independent *M. bovis* BCG cultures onto Middlebrook 7H10 plates containing 0.25 μg of INH/ml and 10 μg of ETH/ml. This double antibiotic selection led to the isolation of mutants at a frequency of 10^{-5} to 10^{-6}. From 15 of the INH^r ETH^r strains sequenced for mutations in the *ndh* gene, 6 were found to possess mutations. Four of the six *ndh* mutants had a single point mutation in the *ndh* gene resulting in amino acid substitutions (Table 2; Fig. 1). The other two had acquired a single base pair insertion, theoretically causing a frameshift in the Ndh open reading frame (Table 2; Fig. 1). The base pair insertions were confirmed by sequencing *ndh* from two independent PCRs using two independent genomic DNA preparations as template. All six mutants displayed low-level resistance phenotypes to INH (2.5- to 6-fold), ETH (4- to 8-fold), and TRC (2- to 3-fold) (Table 2; Fig. 2A). Wild-type susceptibilities to INH, ETH, and TRC could be restored in each mutant by complementation with the wild-type *M. bovis* BCG *ndh* gene (data not shown). This suggests that resistance to all three drugs was directly mediated by mutations within the *ndh* gene in *M. bovis* BCG. Notably, all six *ndh* mutants had no growth defect in liquid medium without antibiotic (Fig. 2B).

Coresistance to INH and ETH in *ndh* mutants is not due to InhA overexpression. Since previous studies had demonstrated that overexpression of *inhA* conferred coresistance to INH and ETH in *M. smegmatis*, *M. bovis* BCG, and *M. tuberculosis* (1, 26), we hypothesized that the coresistance to INH and ETH could be mediated by the up-regulation of *inhA*. To test this hypothesis, the amounts of InhA protein in three *M. bovis* BCG *ndh* mutants (mc^{2}2401, mc^{2}2402, and mc^{2}2403) were

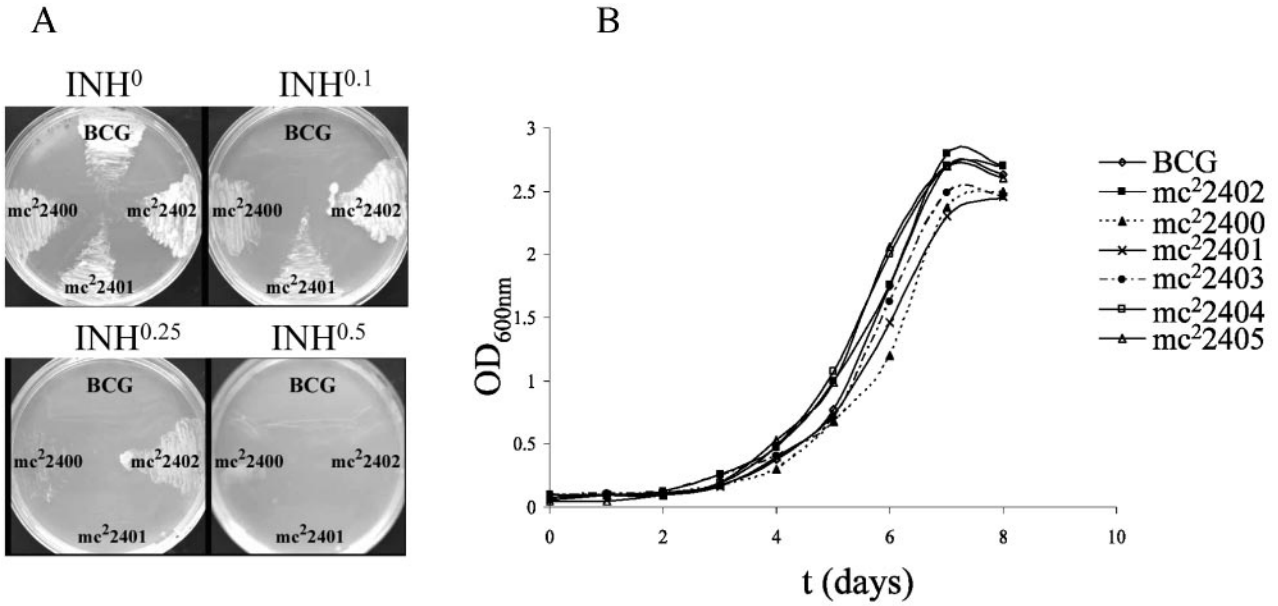

FIG. 2. Growth of *M. bovis* BCG Pasteur *ndh* mutants at 37°C. (A) Growth on solid media containing different concentrations (in micrograms per milliliter) of INH of three *M. bovis* BCG *ndh* mutants (mc^{2}2400, mc^{2}2401, and mc^{2}2402). (B) The *ndh* mutants and parent strain were grown in Middlebrook 7H9 broth supplemented with 10% OADC, 0.2% glycerol, and 0.05% Tween 80. The growth of the cultures was followed spectrophotometrically by measuring the OD_{600}.

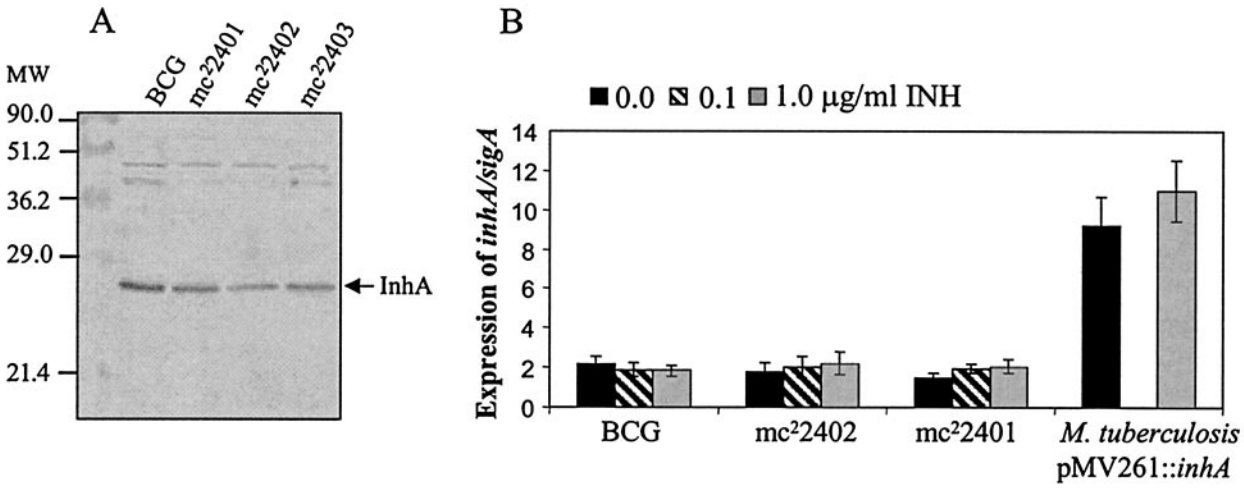

FIG. 3. InhA expression in *ndh* mutants. (A) Western blot analysis. Detection of InhA in total protein extracts obtained from the different *M. bovis* BCG strains using rabbit anti-InhA antibodies raised against the *M. tuberculosis* InhA protein. (B) *inhA* mRNA levels in *M. bovis* BCG strains and the *M. tuberculosis* pMV261::*inhA* strain without addition of INH and after 4 h of incubation in the presence of 0.1 or 1.0 μg of INH/ml. *inhA* values were normalized using *sigA* levels as reference (26). Each value is the average of three culture replicates, each of which was evaluated three times. Error bars correspond to 95% confidence intervals. As a positive control of *inhA* overexpression, the *M. tuberculosis* strain harboring pMV261::*inhA* is shown (26), tested only without antibiotic and 1.0 μg of INH/ml.

compared to that of the parental *M. bovis* BCG strain by Western blot analysis using rabbit anti-InhA antibodies. This analysis showed no significant differences in InhA protein levels between the wild-type strain and the three *M. bovis* BCG *ndh* mutants (Fig. 3A). A further quantification of *inhA* was performed at a transcriptional level in two independent *M. bovis* BCG mutants (mc^{2}2401 and mc^{2}2402) using a molecular beacon mRNA assay (26) in the absence or presence of INH. Figure 3B shows that the level of *inhA* mRNA was similar in all strains tested, thus confirming the results obtained by immunoblotting. This rules out the possibility that coresistance to INH and ETH in the *ndh M. bovis* BCG mutants is mediated by higher InhA levels. Moreover, no increase in the levels of *inhA* mRNA was observed in the various strains, independent of the concentration of INH used (0, 0.1, or 1 μg/ml) (Fig. 3B). In contrast, *M. tuberculosis* transformed with pMV261::*inhA*, which has been previously shown to be coresistant to INH and ETH (26), showed a five- to sixfold increase in *inhA* mRNA levels. From these studies, we conclude that the coresistance to INH and ETH in the *ndh* mutants did not result from increased levels of *inhA* expression.

The *ndh* mutants are defective in NdhII activity. The identification of mutations in *ndh* suggested that the strains would be defective in NdhII activity. Therefore, the NdhII enzymatic activities were determined in the membrane fractions of the unique *ndh* mutants and six complemented mutants by measuring the rate of NADH oxidation in presence of menadione (Table 3; Fig. 4). In *M. smegmatis*, the level of NdhII activity of the different *ndh* mutants ranged from 5 to 48% of the activity of the wild-type strain, mc^{2}155. In *M. bovis* BCG, all six *M. bovis* BCG *ndh* mutants lost between 75 and 90% of their NdhII activity (Fig. 4A). For comparison, we measured the NdhII activity in an INH^r *M. bovis* BCG mutant having a single point mutation in *katG* (G985T, resulting in an Asp329Tyr amino acid change) and found it similar to that of the wild type (Fig. 4A). Complementation with pMV261::*ndh* restored NdhII activity in the mutants from both species to wild-type levels, suggesting that overexpression of a wild-type *ndh* gene could functionally restore the defect of NdhII activity in the mutants (Table 3; Fig. 4B).

The NdhI activity was also assayed by measuring the rate of DCIP reduction in the presence of NHDH, as we were not able to measure the rate of NHDH oxidation in the presence of menadione. The NdhI activity was on average 95% lower than the NdhII activity (assayed by measuring the rate of DCIP reduction in the presence of NADH) in *M. smegmatis* mc^{2}155 and 75% lower in wild-type *M. bovis* BCG. The *M. smegmatis* and *M. bovis* BCG *ndh* mutants had an NdhI activity comparable to that of the wild-type strains (data not shown).

***ndh* mutations result in altered NADH/NAD$^+$ ratios in cells.** Since NdhII encoded by *ndh* oxidizes NADH into NAD$^+$, we reasoned that the mutants with lowered NADH dehydrogenase activity would have an altered NADH/NAD$^+$ ratio in the cells. To test this hypothesis, both intracellular NADH and NAD$^+$ concentrations were measured using a sensitive cycling assay (30). Each mutant was grown at permissive temperature in broth containing neither INH nor ETH in a culture flask fully aerated. The NADH and NAD$^+$ levels were found to be highly dependent on the density of the culture in that higher levels of NADH and NAD$^+$ were measured in denser cultures (data not shown). Nevertheless, our results repeatedly showed that the NADH/NAD$^+$ ratio was significantly higher in the *ndh* mutants than in wild-type *M. smegmatis* or *M. bovis* BCG (NADH/NAD$^+$ $\approx$ 0.7 in parent strains and $\geq$1.0 in the *ndh* mutants; $P < 0.002$). The significance was determined using the Student *t* test (Table 3; Fig. 5A). As expected, in the *M. bovis* BCG INH^r *katG* mutant which had no defect in NdhII, the NADH/NAD$^+$ ratio was similar to that of the wild type (Fig. 5A). In *M. bovis* BCG, we observed that the NAD$^+$ concentrations were comparable in both the wild-type and *ndh* mutants (Fig. 5C). The main difference in these mutants was

TABLE 3. Ndh activity and NADH/NAD^+ ratios in *M. smegmatis* strains

Strain	% Ndh activity[a]	[NADH] (nM)[a]	[NAD^+] (nM)[a]	[NADH]/[NAD^+]
mc^2155	100	1,028 ± 22	1,379 ± 12	0.7
mc^2374	21.0 ± 1.0	1,742 ± 65	1,409 ± 19	1.2
mc^2375	44.8 ± 3.8	1,525 ± 31	1,132 ± 3	1.3
mc^2376	34.0 ± 3.0	2,322 ± 11	1,200 ± 2	1.9
mc^2377	4.8 ± 0.8	1,966 ± 90	1,222 ± 35	1.6
mc^2378	6.8 ± 0.5	1,508 ± 67	836 ± 19	1.8
mc^2379	29.2 ± 4.4	1,129 ± 9	1,100 ± 6	1.0
mc^2380	48.0 ± 2.0	1,760 ± 21	1,502 ± 17	1.2
mc^2381	8.0 ± 0.7	1,728 ± 41	1,116 ± 39	1.5
mc^2382	13.5 ± 0.7	1,845 ± 105	1,335 ± 45	1.4
mc^2383	13.8 ± 0.7	1,505 ± 2	1,113 ± 2	1.4
mc^2384	17.1 ± 2.2	1,268 ± 37	810 ± 5	1.6
mc^2385	15.9 ± 1.5	1,230 ± 105	938 ± 38	1.3
mc^2386	18.1 ± 1.8	1,525 ± 31	1,132 ± 3	1.4
mc^2387	18.2 ± 2.7	1,511 ± 0	1,072 ± 33	1.4
mc^2388	24.0 ± 1.1	1,316 ± 20	870 ± 30	1.5
mc^2155 pMV261	100	987 ± 23	1,372 ± 10	0.7
mc^2155 pMV261::*ndh*	510.4 ± 55.7	362 ± 1	1,056 ± 14	0.3
mc^2378 pMV261	8.6 ± 0.4	3,196 ± 79	1,122 ± 3	2.8
mc^2378 pMV261::*ndh*	841.3 ± 50	587 ± 29	1,098 ± 3	0.5
mc^2381 pMV261	7.9 ± 0.6	2,151 ± 30	1,271 ± 29	1.7
mc^2381 pMV261::*ndh*	584.0 ± 75	577 ± 32	1,280 ± 17	0.4
mc^2377 pMV261	9.7 ± 1.4	2,203 ± 3	950 ± 22	2.3
mc^2377 pMV261::*ndh*	587 ± 66	587 ± 1	1,267 ± 5	0.5

[a] Values are means ± standard deviations.

the NADH concentration, which almost doubled in the *ndh* mutants compared to the wild-type strain (Fig. 5C).

The NADH and NAD^+ concentrations were also measured in *ndh* mutants transformed with the complementing pMV261::*ndh* plasmid (Table 3; Fig. 5B and D). The transformants had an NADH/NAD^+ value (0.4 to 0.5) comparable to that of the wild-type strains transformed with their respective pMV261::*ndh* (0.3). Again, the main change between strains transformed with either pMV261 or pMV261::*ndh* was observed for the NADH concentrations, the NAD^+ concentrations remaining comparable (Table 3; Fig. 5D). Altogether, these results suggest that coresistance to INH and ETH directly correlates with reduced NdhII activity and increased intracellular NADH/NAD^+ ratios.

Increasing NADH concentrations prevent inactivation of InhA by the INH-NAD adduct. Previous studies have established that InhA is an NADH-specific enoyl-ACP reductase (11, 42) that is inhibited by a specific INH-NAD adduct (29, 40, 44, 45, 52). Since we have demonstrated that coresistance to INH and ETH in *ndh* mutants correlates with increased

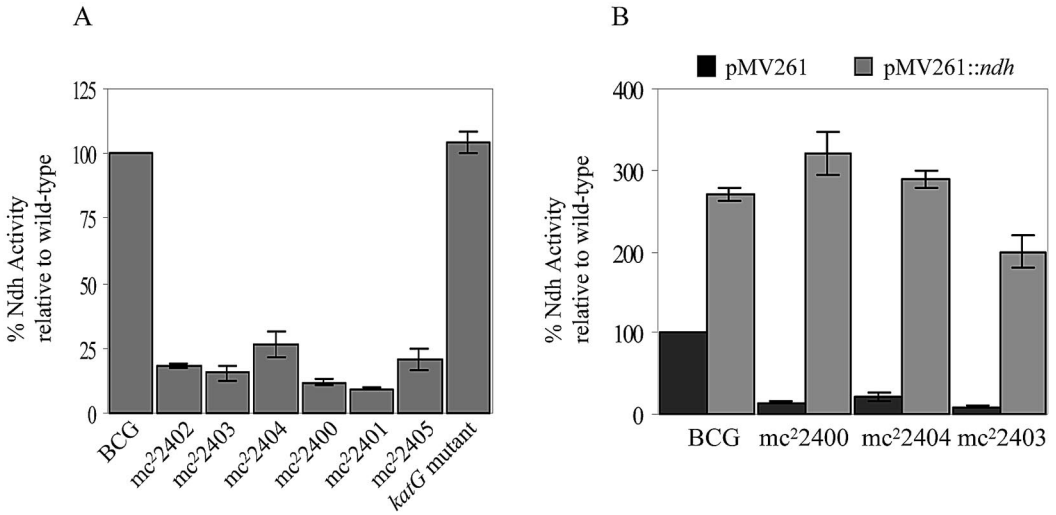

FIG. 4. NADH dehydrogenase activity in *M. bovis* BCG *ndh* mutants and transformants. Ndh activity was measured as described in Materials and Methods and is given as a percentage relative to wild type (either *M. bovis* BCG Pasteur [A] or *M. bovis* BCG Pasteur transformed with pMV261 [B]). For comparison, the Ndh activity of an INH^r *M. bovis* BCG strain having a single point mutation in *katG* (G985T, resulting in an Asp329Tyr amino acid change) is shown. The experiments were repeated three times, and the average is plotted with its standard deviation.

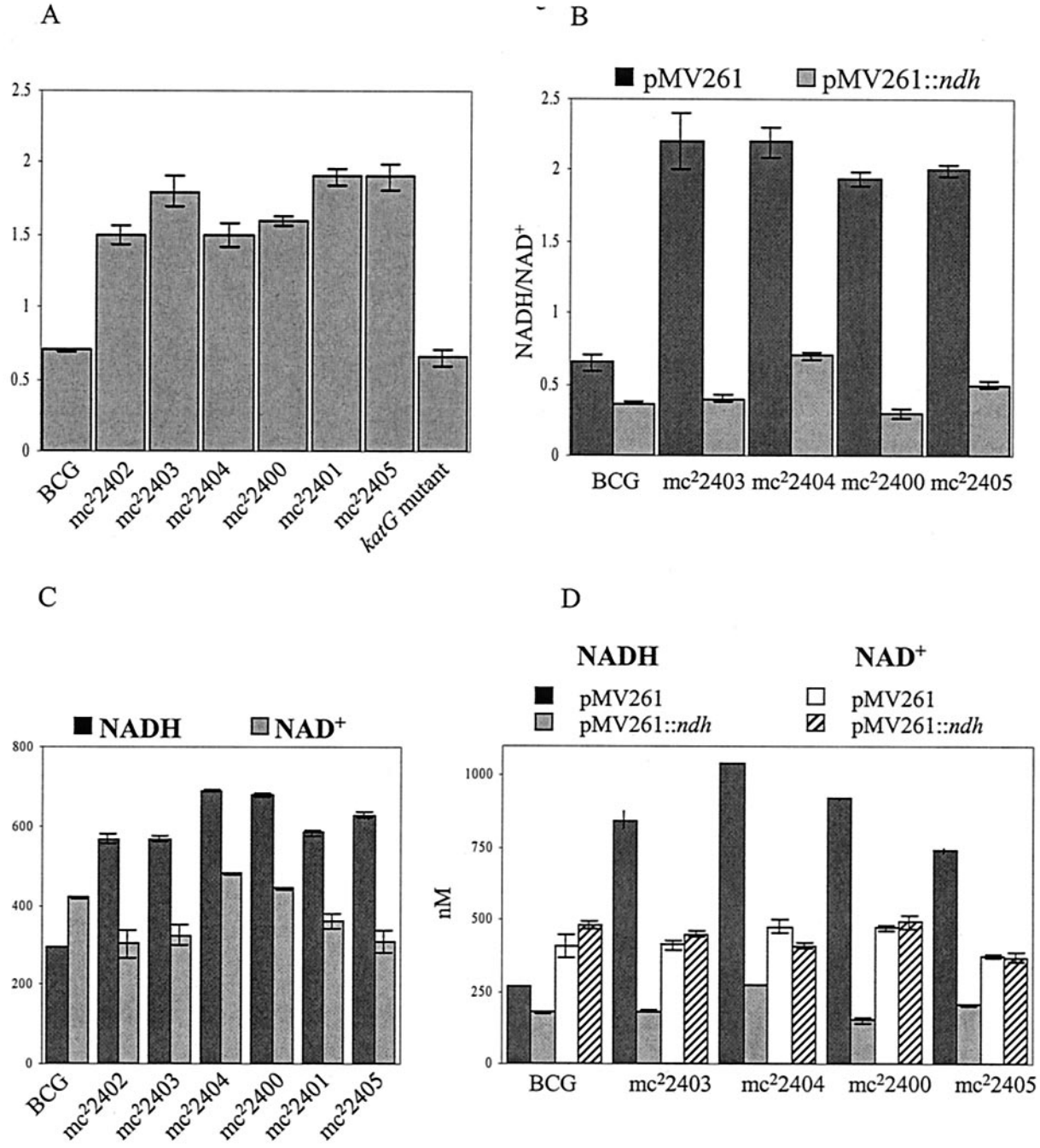

FIG. 5. NADH/NAD$^+$ ratios, NADH concentrations, and NAD$^+$ concentrations in *M. bovis* BCG *ndh* mutants and transformants. The *M. bovis* BCG strains were grown at 37°C to log phase ($OD_{600} \approx 0.8$ to 1). The NADH and NAD$^+$ concentrations were measured in triplicate as described in Materials and Methods. For comparison, the NADH/NAD$^+$ ratio of an INH^r *M. bovis* BCG strain having a single point mutation in *katG* (G985T, resulting in an Asp329Tyr amino acid change) is shown. The experiments were repeated three times, and the average is plotted with its standard deviation.

NADH/NAD$^+$ ratios in the mutant cells, we hypothesized that the increased NADH concentrations mediate resistance by competitively inhibiting the binding of the INH-NAD adduct. Nguyen et al. (40) showed that high concentrations of NADH can prevent inhibition of InhA by the INH-NAD adduct. These authors reported that treatment of InhA with a 100 nM pool of INH-NAD adducts resulted in a 78% loss of InhA activity. However, when InhA was preincubated with 100 μM NADH and then treated with the pool of INH-NAD adducts, no InhA inhibition was observed, suggesting that high concentrations of NADH protect the adduct-mediated inhibition of InhA. To confirm the hypothesis that an excess of NADH could prevent inactivation of InhA by the INH-NAD adduct, the inhibition of InhA by the INH-NAD adduct was tested in the presence of increasing concentrations of NADH under three different conditions in vitro (Fig. 6). In the first two

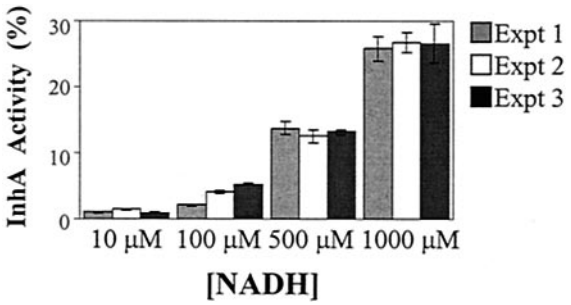

FIG. 6. InhA activity versus NADH concentration. In experiment 1, the INH-NAD adduct was first prepared by adding Mn(III) pyrophosphate (4 mM) into a mixture of INH (2 mM) and NAD^+ (2 mM). InhA (60 nM) and NADH (10, 100, or 500 μM or 1 mM) were preincubated for 20 min prior to the addition of the INH-NAD adduct (10 μM). The reaction was initiated by the addition of 2-*trans*-dodecenoyl-CoA (50 μM). In experiment 2, InhA (60 nM) and NADH (10, 100, 500, or 1,000 μM) were preincubated for 20 min. INH (10 μM) and Mn(III) pyrophosphate (20 μM) were then added. The mixture was incubated for another 5 min before adding 2-*trans*-dodecenoyl-CoA (50 μM). In experiment 3, the INH-NAD adduct was prepared as in experiment 1 and incubated with InhA (5 μM) for 3 h. The inhibited InhA was separated from other components by using a desalting column, and the inhibited InhA (60 nM) was assayed under different concentrations of NADH (10, 100, or 500 μM or 1 mM). In each experiment, the InhA activity was assayed by monitoring the NADH absorption at 340 nm for 2 min, at room temperature, using 2-*trans*-dodecenoyl-CoA (50 μM) as a substrate.

experiments (experiments 1 and 2 in Fig. 6), the enzyme was preincubated with NADH prior to the addition of the inhibitor [either as a preformed INH-NAD adduct or as a mixture of INH and Mn(III) pyrophosphate] and the substrate. In the third experiment, InhA was preincubated with the INH-NAD adduct for 3 h, and activity of the inhibited enzyme was then assayed in the presence of different concentrations of NADH. All three experiments yielded one consistent trend: increasing concentrations of NADH directly correlated with a decrease in the inhibition of InhA by the INH-NAD adduct. Therefore, we can conclude that high levels of NADH can protect InhA from the INH-NAD adduct, resulting in INH resistance.

Specific *ndh* mutations mediate a Ts bactericidal phenotype. To further characterize the different *ndh* alleles, we tested whether incubation at 42°C was a bactericidal or static event in *M. smegmatis ndh* mutants. The mutants were grown at permissive temperature, titers were determined, and 10-fold serial dilutions were plated on plates containing no antibiotic and incubated at 42°C for 4 to 5 days. The plates incubated at 42°C were then shifted to the permissive temperature (30°C) and incubated for another 7 days. The phenotype was considered Ts bactericidal when less than 10% of cells could survive incubation at 42°C. Five *ndh* mutants (*ndh-11* [Leu100Pro], *ndh-32* [Arg145Cys], *ndh-61* [Gly84Asp], *ndh-63* [Arg145Cys], and *ndh-93* [Arg145Cys]) did not survive incubation at 42°C, and the mutations were considered bactericidal. The other mutants did not grow at 42°C but were able to resume growth once the plates were shifted to permissive temperature (30°C). Interestingly, the lowest NdhII activity was observed for the mutants having a Ts bactericidal phenotype ($mc^2$2377, $mc^2$2378, and $mc^2$2381) (Table 3). In broth at nonpermissive temperature (42°C), growth ceased for all bactericidal mutants as well as five static mutants (Fig. 7A). In contrast, the seven other static mutants grew at the nonpermissive temperature, but at a much slower rate than wild-type *M. smegmatis* (Fig. 7B). After 24 h of incubation in Middlebrook 7H9 broth at nonpermissive temperature, the drop in the number of viable cells was less than 1 log for static *ndh* mutants (21 of 26), while the five bactericidal mutants had up to a 3-log drop in viable cells (data not shown). The reduction in viable cells was medium dependent, with maximal decreases in survival in minimal medium compared to results in tryptic soy or Mueller-Hinton broth (data not shown). Interestingly, most of the strains with mutations in the carboxy end of Ndh had no growth defect in medium containing up to 100 μg of INH/ml at the permissive temperature (Fig. 8A), whereas strains with mutations in the amino terminus of Ndh showed a slower growth rate with increasing concentration of INH (Fig. 8B).

DISCUSSION

The analyses of mutations conferring resistance to drugs have been invaluable in elucidating the mechanisms of drug action and drug resistance. The discoveries of the phenotypes demonstrating that inactivation of the *katG* (20, 56, 57) and *ethA* (3, 10, 50) genes conferred resistance to INH and ETH, respectively, established that both INH and ETH are prodrugs with independent activation pathways. Resistance was shown to be mediated by recessive mutations causing a loss of prodrug-activating activities (Fig. 9). Genetic studies demonstrating target overexpression or target alteration revealed that INH and ETH shared a common target, InhA (1, 26). In contrast to the mutations in the INH or ETH activator genes, target mutations are dominant to the wild-type gene. Another mechanism of coresistance to INH and ETH was previously demonstrated to be mediated in *M. smegmatis* in a recessive fashion by mutations in *ndh*, a gene encoding a type II NADH dehydrogenase (36). It was unclear if a similar mechanism could function in slow-growing mycobacteria such as *M. tuberculosis* or *M. bovis* BCG, which are 100 times more sensitive to INH than *M. smegmatis*. Moreover, the precise mechanism by which mutations in *ndh* could mediate coresistance to both INH and ETH was also unclear.

To address these points, in this study 6 *M. bovis* BCG *ndh* mutants and 14 novel *M. smegmatis ndh* mutants coresistant to INH and ETH were isolated. Sequence analysis revealed the presence of specific mutations in the *ndh* gene. To date, no INH^r ETH^r *M. tuberculosis* mutants could be isolated in three independent attempts by directly plating *M. tuberculosis* H37Rv on INH and ETH plates, as done for *M. bovis* BCG (data not shown). We tried to obtain the *ndh* mutant strains found in INH^r clinical isolates of *M. tuberculosis* described previously (27), but these strains were not saved. Our inability to isolate *M. tuberculosis* H37Rv *ndh* mutants might result from the concentrations of drugs used to do the screening for this particular strain, and it may reflect metabolic differences among *M. tuberculosis* strains. Interestingly, Middlebrook and Cohn had described the presence of INH^r mutants that were catalase positive but failed to grow on Middlebrook minimal medium (35). It may be that *ndh* mutants of *M. tuberculosis* are auxotrophic for certain nutrients, as observed for some *M. smegmatis* mutants (36). Further analyses are under way to explore these possibilities. Nevertheless, complementation of

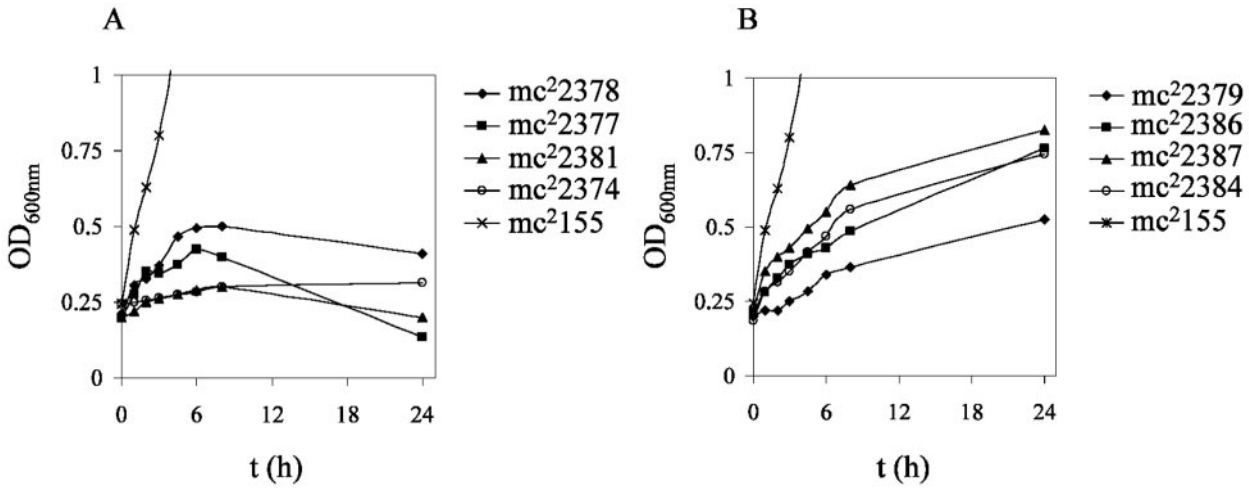

FIG. 7. Effect of nonpermissive temperature (42°C) on *M. smegmatis ndh* Ts mutants in liquid media. The *ndh* mutants were grown at 30°C to mid-log phase, diluted to an OD_{600} of ≈0.2, and shifted to 42°C ($t = 0$). The growth of the cultures was followed spectrophotometrically by measuring the OD_{600}. To simplify the figures, only four mutants are shown per group. (A) Growth was ceased for the following *M. smegmatis ndh* Ts mutants: mc²2374, mc²2375, mc²2376, mc²2377, mc²2378, mc²2381, mc²2383, and mc²2385. (B) Shift to 42°C slows the growth of the following *M. smegmatis ndh* Ts mutants: mc²2379, mc²2380, mc²2382, mc²2384, mc²2386, mc²2387, and mc²2388.

the *M. bovis* BCG *ndh* mutations with the wild-type *M. bovis* BCG *ndh* gene restored full susceptibility to both INH and ETH, proving that these *ndh* mutations were sufficient to mediate the INH and ETH coresistance phenotypes in the *M. tuberculosis* complex.

The phenotype of coresistance mediated by mutations in *inhA* and *ndh* suggests that both INH and ETH target a common enzyme, InhA, and share a common mechanism of action. To address the molecular mechanism of resistance mediated by the *ndh* mutations, we first looked at the possibility that *ndh* mutations mediate coresistance to INH and ETH by overexpressing *inhA*. Using a quantitative PCR test, we were able to establish that the levels of *inhA* were not increased in the *M. bovis* BCG mutants analyzed. This was further confirmed at a translational level by Western blotting.

It was previously postulated that an NdhII defect in *M. smegmatis* would result in an altered $NADH/NAD^+$ ratio due to an increase in the NADH concentration, which would prevent InhA inhibition (36, 45). To test this hypothesis, the $NADH/NAD^+$ ratios were measured in all the *M. bovis* BCG and *M. smegmatis ndh* mutants and found to be greater than 1.0 in *M. smegmatis* and greater than 1.6 in *M. bovis* BCG, compared to 0.7 for the wild-type strains. In fact, the increase in the $NADH/NAD^+$ ratios was mostly due to an increase in

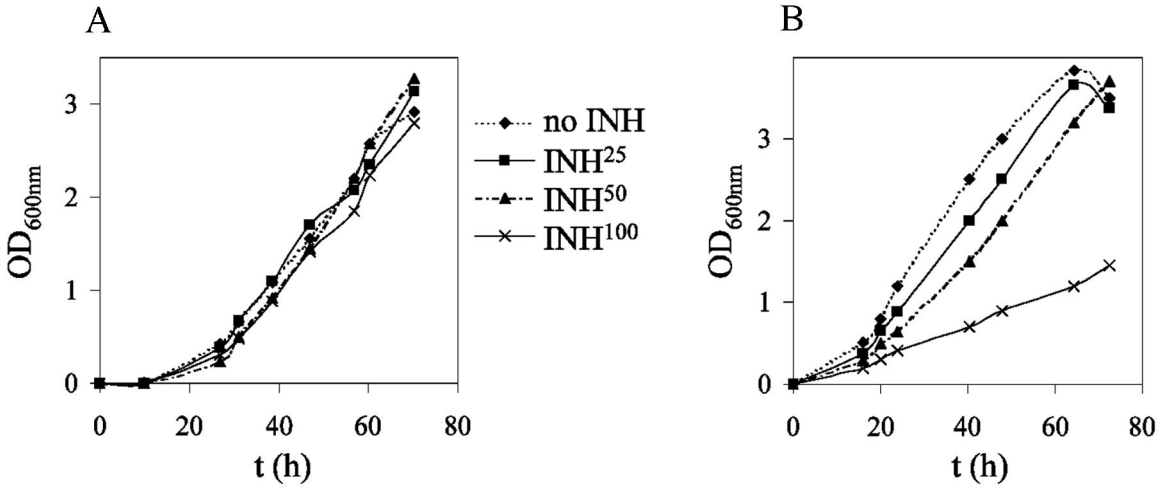

FIG. 8. Growth of *M. smegmatis ndh* mutants at permissive temperature (30°C) with and without INH. The *ndh* mutants were grown at 30°C to mid-log phase and diluted to an OD_{600} of ≈0.05. The diluted cultures (10 ml) were added to four square bottles, and to each square bottle was added 0, 25, 50, or 100 μg of INH/ml. The cultures were incubated while shaking at 30°C. The growth of the cultures was followed spectrophotometrically by measuring the OD_{600}. To simplify the figures, only one mutant is shown per group. (A) Typical growth curve for *M. smegmatis ndh* mutants not affected by INH, such as mc²2374, mc²2376, mc²2378, mc²2379, mc²2380, mc²2381, and mc²2384 (mutant shown is mc²2384). (B) Typical growth curves of *M. smegmatis ndh* mutants with a growth rate delayed by INH, such as mc²2375, mc²2377, mc²2382, mc²2383, mc²2385, mc²2386, mc²2387, and mc²2388 (mutant shown is mc²2377).

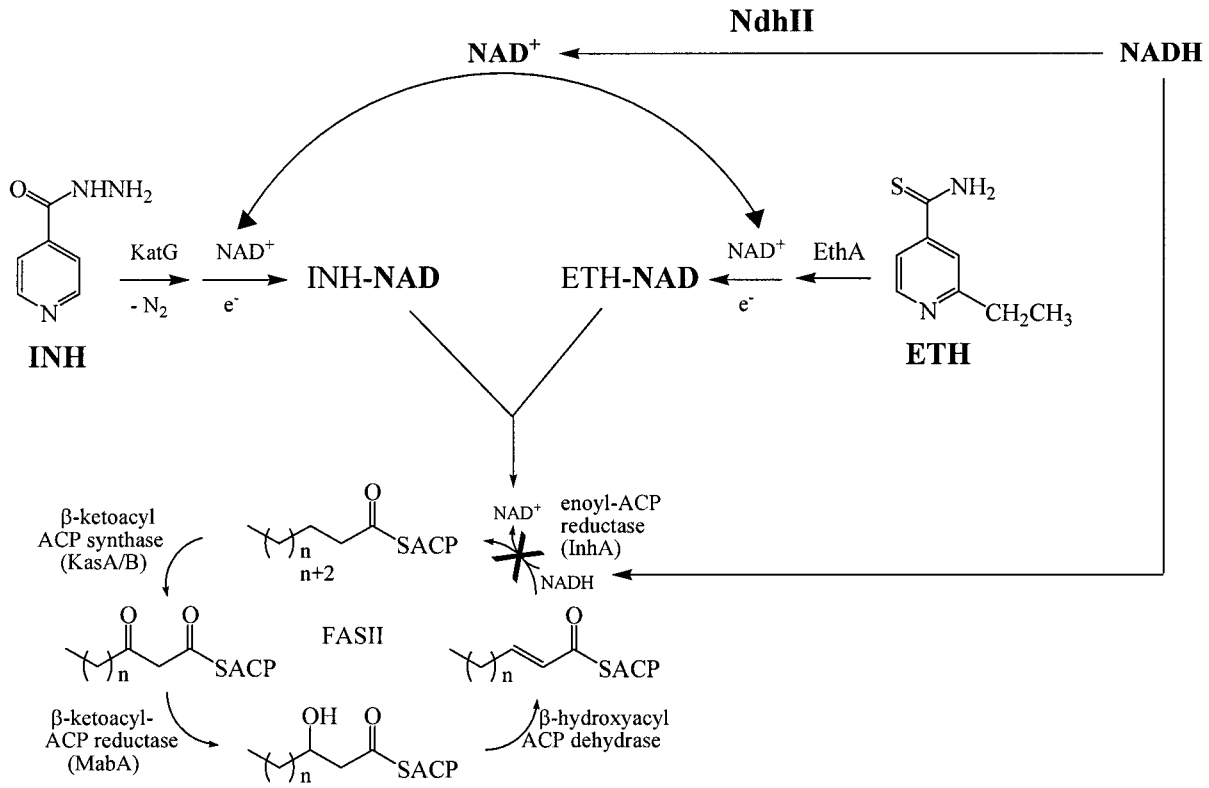

Genes with alleles that transfer resistance or susceptibility to INH or ETH upon transformation

	INH resistance	ETH resistance
katG	+	-
ethA	-	+
inhA	+	+
ndh	+	+

FIG. 9. Proposed mechanism of action of INH and ETH. INH and ETH are both prodrugs that are activated by the catalase-peroxidase KatG or the monooxygenase EthA, respectively. The activated forms react with NAD^+ to form an INH-NAD or ETH-NAD adduct. These adducts inhibit the common target InhA, the NADH-dependent enoyl-ACP reductase of the fatty acid synthase type II system, resulting in mycolic acid biosynthesis inhibition and cell lysis. Resistance to INH or ETH is associated with recessive mutations in the genes encoding the activators of the drugs, *katG* and *ethA*, respectively, which prevent drug activation. Coresistance to INH and ETH is associated with dominant mutations in the gene encoding the common target of the drugs, *inhA*, which result in target amplification or target modification. A novel mechanism of coresistance to INH and ETH is by recessive mutations in *ndh*, which increase the NADH intracellular concentration and cause resistance by competitively inhibiting the binding of the INH-NAD or ETH-NAD adduct to InhA. This working model accounts for all known resistance phenotypes that have been transferred from drug-sensitive to drug-resistant strains to date.

the NADH concentration. Nguyen et al. (40) first showed that preincubation of InhA with NADH prevented inhibition of InhA by the INH-NAD adduct. Our in vitro biochemical assays showed that increasing concentrations of NADH competitively inhibit binding of the INH-NAD adduct to InhA, irrespective of the order of addition of the different substrates or inhibitors to the InhA enzyme. Although the concentrations of NADH in these experiments are higher than the intracellular physiological concentrations present in the cells, it is unclear what the localized concentrations of NADH and INH-NAD adduct might be for InhA. The in vitro trend of protection from inhibition is fully consistent with the intracellular NADH increase observed for all *ndh* mutants. Therefore, we conclude that increased NADH/NAD^+ ratios most likely competitively inhibit the binding of the INH-NAD or ETH-NAD adduct to InhA, thus resulting in INH and ETH resistance.

An alternative hypothesis was that the altered NADH/NAD^+ ratios reduced or inhibited the activities of KatG and

EthA, the activators of INH and ETH, respectively. However, Miesel et al. (36) showed that *M. smegmatis ndh* mutations causing INH resistance did not result in decreased KatG expression. Moreover, Fraaije et al. (14) reported that EthA, a FAD-containing monooxygenase, uses NADPH and not NADH as a cofactor. Thus, it appears that a high concentration of NADH does not prevent activation of INH or ETH.

We conclude that both INH and ETH are prodrugs which, when activated, form adducts with NAD, and the resulting INH-NAD and ETH-NAD adducts inactivate InhA (Fig. 9). We further conclude that InhA is the single primary target of action for both INH and ETH. Low-level resistance to these drugs is mediated by altering the NADH/NAD^+ ratios. This alteration might be mediated by other metabolic enzymes than NdhII. Supporting this premise, the *M. bovis* BCG mutants isolated in our screen, which are coresistant to INH and ETH but have no mutations in *ndh* (see Results), have altered NADH/NAD^+ ratios (C. Vilchèze and W. R. Jacobs, Jr., unpublished results). Efforts are under way to genetically identify the mutated genes in these strains. In addition, a number of clinical isolates of *M. tuberculosis* have been identified which are resistant to INH or coresistant to INH and ETH and possess no mutations in either *inhA* or *ndh* (38, 43). We postulate that such mutations could (i) mediate overexpression of *inhA*, (ii) alter *ndh* expression levels, or (iii) metabolically alter the NADH/NAD^+ ratios. The *mdh* gene represents such a candidate (36), as well as the *glf* and *ceoBC* genes, which may contribute to INH resistance (8). Interestingly, the products of the *glf* and *ceoBC* genes are NAD^+ binding proteins. Furthermore, mutations altering the NADH/NAD^+ ratio might provide useful tools to elucidate key regulators of energy metabolism in this postgenomic era of biology.

The role that NdhII plays in cell metabolism has been unclear, but it has been proposed that NdhII might control the NADH pool to regulate cell energy metabolism (5, 16, 39). INH^r ETH^r *M. smegmatis* and *M. bovis* BCG *ndh* mutants have defective NdhII activity, resulting in altered NADH/NAD^+ ratios. Complementation of the mutants with a wild-type *ndh* gene restored drug sensitivity, NdhII activity, and a NADH/NAD^+ ratio similar to wild type. Therefore, it appears that NdhII is a major regulator of the NADH/NAD^+ ratio in cells during exponential, aerobic growth for both fast- and slow-growing mycobacteria. The mutations that cause the reduced NdhII activity are distributed throughout the first 80% of the protein. Interestingly, according to the TransMembrane Hidden Markov model algorithm website (http://www.cbs.dtu.dk/services/TMHMM/), which predicts transmembrane domains, the NdhII protein of *Mycobacterium* species and related *Corynebacterium* contains a single transmembrane-spanning region, a region where no mutations have yet to be observed (Fig. 1). In contrast to the *E. coli* enzyme, which has been characterized as a membrane-bound protein, the mycobacterial NdhII enzyme appears to be membrane associated. Interestingly, all the mutations in *ndh* in *M. smegmatis* confer a Ts phenotype to the growth of *M. smegmatis*. The numbers of independent mutants isolated to date (Fig. 1) would argue that the Ts phenotype results not from Ts NdhII activity but rather from a conditional growth arrest caused by the altered NADH/NAD^+ ratio, stabilizing activity. Certain mutants in *ndh* have been shown to lead to auxotrophies (36), suggesting that altered NADH/NAD^+ ratios do affect overall metabolism, a reasonable expectation for the important electron donor NADH.

The mutations that alter NdhII activity from *M. smegmatis* could be readily classified based on their Ts phenotypes, which allowed us to test if thermal inactivation was either a bacteriostatic or bactericidal event. A set of mutations (Gly84Asp, Leu100Pro, and Arg145Cys), found in the region between the FAD and NAD binding sites, conferred a bactericidal effect upon inactivation. We believe that the development of compounds that target this NdhII region could lead to novel bactericidal drugs against mycobacterial pathogens. Further work to characterize these bactericidal biochemical events following thermal inactivation may provide insight into a novel mechanism by which mycobacterial cells die, thereby providing a rationale for designing better antimycobacterial drugs.

ACKNOWLEDGMENTS

This work was supported by NIH grants AI43268 and AI46669. L.K. is supported by INSERM. J.C.S. is supported by the Welch foundation.

We thank Yossef Av-Gay for the critical reading of the manuscript and engaging discussion.

REFERENCES

1. **Banerjee, A., E. Dubnau, A. Quemard, V. Balasubramanian, K. S. Um, T. Wilson, D. Collins, G. de Lisle, and W. R. Jacobs, Jr.** 1994. *inhA*, a gene encoding a target for isoniazid and ethionamide in *Mycobacterium tuberculosis*. Science **263:**227–230.
2. **Basso, L. A., R. Zheng, J. M. Musser, W. R. Jacobs, Jr., and J. S. Blanchard.** 1998. Mechanisms of isoniazid resistance in *Mycobacterium tuberculosis*: enzymatic characterization of enoyl reductase mutants identified in isoniazid-resistant clinical isolates. J. Infect. Dis. **178:**769–775.
3. **Baulard, A. R., J. C. Betts, J. Engohang-Ndong, S. Quan, R. A. McAdam, P. J. Brennan, C. Locht, and G. S. Besra.** 2000. Activation of the pro-drug ethionamide is regulated in mycobacteria. J. Biol. Chem. **275:**28326–28331.
4. **Bernstein, J. W., A. Lott, B. A. Steinberg, and H. L. Yale.** 1952. Chemotherapy of experimental tuberculosis. Am. Rev. Tuberc. **65:**357–374.
5. **Calhoun, M. W., K. L. Oden, R. B. Gennis, M. J. de Mattos, and O. M. Neijssel.** 1993. Energetic efficiency of *Escherichia coli*: effects of mutations in components of the aerobic respiratory chain. J. Bacteriol. **175:**3020–3025.
6. **Canetti, G.** 1965. Present aspects of bacterial resistance in tuberculosis. Am. Rev. Respir. Dis. **92:**687–703.
7. **Canetti, G., B. Kreis, R. G. Thibier, and M. P. Le Lirzin.** 1967. Current data on primary resistance in pulmonary tuberculosis in adults in France. 2d survey of the Centre d'Etudes sur la Resistance Primaire: 1965–1966. Rev. Tuberc. Pneumol. (Paris) **31:**433–474.
8. **Chen, P., and W. R. Bishai.** 1998. Novel selection for isoniazid (INH) resistance genes supports a role for NAD^+-binding proteins in mycobacterial INH resistance. Infect. Immun. **66:**5099–5106.
9. **Corbett, E. L., C. J. Watt, N. Walker, D. Maher, B. G. Williams, M. C. Raviglione, and C. Dye.** 2003. The growing burden of tuberculosis: global trends and interactions with the HIV epidemic. Arch. Intern. Med. **163:**1009–1021.
10. **DeBarber, A. E., K. Mdluli, M. Bosman, L. G. Bekker, and C. E. Barry III.** 2000. Ethionamide activation and sensitivity in multidrug-resistant *Mycobacterium tuberculosis*. Proc. Natl. Acad. Sci. USA **97:**9677–9682.
11. **Dessen, A., A. Quemard, J. S. Blanchard, W. R. Jacobs, Jr., and J. C. Sacchettini.** 1995. Crystal structure and function of the isoniazid target of *Mycobacterium tuberculosis*. Science **267:**1638–1641.
12. **Espinal, M. A.** 2003. The global situation of MDR-TB. Tuberculosis **83:**44–51.
13. **Fox, H. H.** 1952. The chemical approach to the control of tuberculosis. Science **116:**129–134.
14. **Fraaije, M. W., N. M. Kamerbeek, A. J. Heidekamp, R. Fortin, and D. B. Janssen.** 2004. The prodrug activator EtaA from *Mycobacterium tuberculosis* is a Baeyer-Villiger monooxygenase. J. Biol. Chem. **279:**3354–3360.
15. **Gennis, R. B., and V. Stewart.** 1996. Respiration, p. 217–261. *In* F. C. Neidhardt, R. Curtiss III, J. L. Ingraham, E. C. C. Lin, K. B. Low, B. Magasanik, W. S. Reznikoff, M. Riley, M. Schaechter, and H. E. Umbarger (ed.), *Escherichia coli* and *Salmonella*: cellular and molecular biology, vol. 1. ASM Press, Washington, D.C.
16. **Green, J., and J. R. Guest.** 1994. Regulation of transcription at the *ndh* promoter of *Escherichia coli* by FNR and novel factors. Mol. Microbiol. **12:**433–444.
17. **Heym, B., N. Honore, C. Truffot-Pernot, A. Banerjee, C. Schurra, W. R.**

Jacobs, Jr., J. D. van Embden, J. H. Grosset, and S. T. Cole. 1994. Implications of multidrug resistance for the future of short-course chemotherapy of tuberculosis: a molecular study. Lancet **344:**293–298.
18. **Hok, T. T.** 1964. A comparative study of the susceptibility to ethionamide, thiosemicarbazone, and isoniazid of tubercle bacilli from patients never treated with ethionamide or thiosemicarbazone. Am. Rev. Respir. Dis. **90:** 468–469.
19. **Jaworowski, A., G. Mayo, D. C. Shaw, H. D. Campbell, and I. G. Young.** 1981. Characterization of the respiratory NADH dehydrogenase of *Escherichia coli* and reconstitution of NADH oxidase in *ndh* mutant membrane vesicles. Biochemistry **20:**3621–3628.
20. **Johnsson, K., and P. G. Schultz.** 1994. Mechanistic studies of the oxidation of isoniazid by the catalase peroxidase from *Mycobacterium tuberculosis*. J. Am. Chem. Soc. **116:**7425–7426.
21. **Kerscher, S. J.** 2000. Diversity and origin of alternative NADH:ubiquinone oxidoreductases. Biochim. Biophys. Acta **1459:**274–283.
22. **Kiepiela, P., K. S. Bishop, A. N. Smith, L. Roux, and D. F. York.** 2000. Genomic mutations in the *katG*, *inhA* and *aphC* genes are useful for the prediction of isoniazid resistance in *Mycobacterium tuberculosis* isolates from Kwazulu Natal, South Africa. Tuberc. Lung Dis. **80:**47–56.
23. **Kremer, L., L. G. Dover, H. R. Morbidoni, C. Vilcheze, W. N. Maughan, A. Baulard, S. Tu, N. Honore, V. Deretic, J. C. Sacchettini, C. Locht, W. R. J. Jacobs, and G. Besra.** 2003. Inhibition of InhA activity, but not KasA activity, induces formation of a KasA-containing complex in mycobacteria. J. Biol. Chem. **278:**20547–20554.
24. **Laemmli, U. K.** 1970. Cleavage of structural proteins during the assembly of the head of bacteriophage T4. Nature **227:**680–685.
25. **Larsen, M. H.** 2000. Some common methods in mycobacterial genetics, p. 313–320. *In* G. F. Hatfull and W. R. Jacobs, Jr. (ed.), Molecular genetics of mycobacteria. ASM Press, Washington, D.C.
26. **Larsen, M. H., C. Vilcheze, L. Kremer, G. S. Besra, L. Parsons, M. Salfinger, L. Heifets, M. H. Hazbon, D. Alland, J. C. Sacchettini, and W. R. Jacobs, Jr.** 2002. Overexpression of *inhA*, but not *kasA*, confers resistance to isoniazid and ethionamide in *Mycobacterium smegmatis*, *M. bovis* BCG and *M. tuberculosis*. Mol. Microbiol. **46:**453–466.
27. **Lee, A. S., A. S. Teo, and S. Y. Wong.** 2001. Novel mutations in *ndh* in isoniazid-resistant *Mycobacterium tuberculosis* isolates. Antimicrob. Agents Chemother. **45:**2157–2159.
28. **Lefford, M. J.** 1966. The ethionamide sensitivity of British pre-treatment strains of *Mycobacterium tuberculosis*. Tubercle **47:**198–206.
29. **Lei, B., C. J. Wei, and S. C. Tu.** 2000. Action mechanism of antitubercular isoniazid. Activation by *Mycobacterium tuberculosis* KatG, isolation, and characterization of *inha* inhibitor. J. Biol. Chem. **275:**2520–2526.
30. **Leonardo, M. R., Y. Dailly, and D. P. Clark.** 1996. Role of NAD in regulating the *adhE* gene of *Escherichia coli*. J. Bacteriol. **178:**6013–6018.
31. **Madison, B. M., S. H. Siddiqi, L. Heifets, W. Gross, M. Higgins, N. Warren, A. Thompson, G. Morlock, and J. C. Ridderhof.** 2004. Identification of a *Mycobacterium tuberculosis* strain with stable, low-level resistance to isoniazid. J. Clin. Microbiol. **42:**1294–1295.
32. **Matsushita, K., T. Ohnishi, and H. R. Kaback.** 1987. NADH-ubiquinone oxidoreductases of the *Escherichia coli* aerobic respiratory chain. Biochemistry **26:**7732–7737.
33. **McKie, J. H., and K. T. Douglas.** 1991. Evidence for gene duplication forming similar binding folds for NAD(P)H and FAD in pyridine nucleotide-dependent flavoenzymes. FEBS Lett. **279:**5–8.
34. **McMurry, L. M., P. F. McDermott, and S. B. Levy.** 1999. Genetic evidence that InhA of *Mycobacterium smegmatis* is a target for triclosan. Antimicrob. Agents Chemother. **43:**711–713.
35. **Middlebrook, G., and M. L. Cohn.** 1953. Some observations on the pathogenicity of isoniazid-resistant variants of tubercle bacilli. Science **118:**297–299.
36. **Miesel, L., T. R. Weisbrod, J. A. Marcinkeviciene, R. Bittman, and W. R. Jacobs, Jr.** 1998. NADH dehydrogenase defects confer isoniazid resistance and conditional lethality in *Mycobacterium smegmatis*. J. Bacteriol. **180:**2459–2467.
37. **Molenaar, D., M. E. van der Rest, A. Drysch, and R. Yucel.** 2000. Functions of the membrane-associated and cytoplasmic malate dehydrogenases in the citric acid cycle of *Corynebacterium glutamicum*. J. Bacteriol. **182:**6884–6891.
38. **Morlock, G. P., B. Metchock, D. Sikes, J. T. Crawford, and R. C. Cooksey.** 2003. *ethA*, *inhA*, and *katG* loci of ethionamide-resistant clinical *Mycobacterium tuberculosis* isolates. Antimicrob. Agents Chemother. **47:**3799–3805.
39. **Neijssel, O. M., and M. J. Teixeira de Mattos.** 1994. The energetics of bacterial growth: a reassessment. Mol. Microbiol. **13:**172–182.
40. **Nguyen, M., A. Quemard, S. Broussy, J. Bernadou, and B. Meunier.** 2002. Mn(III) pyrophosphate as an efficient tool for studying the mode of action of isoniazid on the InhA protein of *Mycobacterium tuberculosis*. Antimicrob. Agents Chemother. **46:**2137–2144.
41. **Piatek, A. S., A. Telenti, M. R. Murray, H. El-Hajj, W. R. Jacobs, Jr., F. R. Kramer, and D. Alland.** 2000. Genotypic analysis of *Mycobacterium tuberculosis* in two distinct populations using molecular beacons: implications for rapid susceptibility testing. Antimicrob. Agents Chemother. **44:**103–110.
42. **Quemard, A., J. C. Sacchettini, A. Dessen, C. Vilcheze, R. Bittman, W. R. Jacobs, Jr., and J. S. Blanchard.** 1995. Enzymatic characterization of the target for isoniazid in *Mycobacterium tuberculosis*. Biochemistry **34:**8235–8241.
43. **Ramaswamy, S. V., R. Reich, S. J. Dou, L. Jasperse, X. Pan, A. Wanger, T. Quitugua, and E. A. Graviss.** 2003. Single nucleotide polymorphisms in genes associated with isoniazid resistance in *Mycobacterium tuberculosis*. Antimicrob. Agents Chemother. **47:**1241–1250.
44. **Rawat, R., A. Whitty, and P. J. Tonge.** 2003. The isoniazid-NAD adduct is a slow, tight-binding inhibitor of InhA, the *Mycobacterium tuberculosis* enoyl reductase: adduct affinity and drug resistance. Proc. Natl. Acad. Sci. USA **100:**13881–13886.
45. **Rozwarski, D. A., G. A. Grant, D. H. Barton, W. R. Jacobs, Jr., and J. C. Sacchettini.** 1998. Modification of the NADH of the isoniazid target (InhA) from *Mycobacterium tuberculosis*. Science **279:**98–102.
46. **San, K. Y., G. N. Bennett, S. J. Berrios-Rivera, R. V. Vadali, Y. T. Yang, E. Horton, F. B. Rudolph, B. Sariyar, and K. Blackwood.** 2002. Metabolic engineering through cofactor manipulation and its effects on metabolic flux redistribution in *Escherichia coli*. Metab. Eng. **4:**182–192.
47. **Sonnhammer, E. L., G. von Heijne, and A. Krogh.** 1998. A hidden Markov model for predicting transmembrane helices in protein sequences. Proc. Int. Conf. Intell. Syst. Mol. Biol. **6:**175–182.
48. **Stover, C. K., V. F. de la Cruz, T. R. Fuerst, J. E. Burlein, L. A. Benson, L. T. Bennett, G. P. Bansal, J. F. Young, M. H. Lee, G. F. Hatfull, et al.** 1991. New use of BCG for recombinant vaccines. Nature **351:**456–460.
49. **Takayama, K., L. Wang, and H. L. David.** 1972. Effect of isoniazid on the in vivo mycolic acid synthesis, cell growth, and viability of *Mycobacterium tuberculosis*. Antimicrob. Agents Chemother. **2:**29–35.
50. **Vannelli, T. A., A. Dykman, and P. R. Ortiz de Montellano.** 2002. The antituberculosis drug ethionamide is activated by a flavoprotein monooxygenase. J. Biol. Chem. **277:**12824–12829.
51. **Vilcheze, C., H. R. Morbidoni, T. R. Weisbrod, H. Iwamoto, M. Kuo, J. C. Sacchettini, and W. R. Jacobs, Jr.** 2000. Inactivation of the *inhA*-encoded fatty acid synthase II (FASII) enoyl-acyl carrier protein reductase induces accumulation of the FASI end products and cell lysis of *Mycobacterium smegmatis*. J. Bacteriol. **182:**4059–4067.
52. **Wilming, M., and K. Johnsson.** 1999. Spontaneous formation of the bioactive form of the tuberculosis drug isoniazid. Angew Chem. Int. Ed. **38:**2588–2590.
53. **World Health Organization.** 2000. Anti-tuberculosis drug resistance in the world. Report no. 2: prevalence and trends. The W.H.O./IUATLD global project on anti-tuberculosis drug resistance surveillance. World Health Organization, Geneva, Switzerland.
54. **Yagi, T.** 1993. The bacterial energy-transducing NADH-quinone oxidoreductases. Biochim. Biophys. Acta **1141:**1–17.
55. **Yagi, T., T. Yano, S. Di Bernardo, and A. Matsuno-Yagi.** 1998. Procaryotic complex I (NDH-1), an overview. Biochim. Biophys. Acta **1364:**125–133.
56. **Zhang, Y., T. Garbe, and D. Young.** 1993. Transformation with *katG* restores isoniazid sensitivity in *Mycobacterium tuberculosis* isolates resistant to a range of drug concentrations. Mol. Microbiol. **8:**521–524.
57. **Zhang, Y., B. Heym, B. Allen, D. Young, and S. Cole.** 1992. The catalase-peroxidase gene and isoniazid resistance of *Mycobacterium tuberculosis*. Nature **358:**591–593.